Nickel(II) and iron(III) selective off-on-type fluorescence probes based on perylene tetracarboxylic diimide†‡

Haixia Wang,[a,b] Delou Wang,[a] Qi Wang,[c] Xiyou Li*[a] and Christoph A. Schalley*[c]

Received 13th October 2009, Accepted 20th November 2009
First published as an Advance Article on the web 5th January 2010
DOI: 10.1039/b921342b

Two novel "turn-on" fluorescent probes with perylene tetracarboxylic diimide (PDI) as the fluorophore and two different di-(2-picolyl)-amine (DPA) groups as the metal ion receptor (**PDI-1** and **PDI-2**) were successfully synthesized with satisfactory yields. **PDI-1** exhibited high selectivity toward Ni^{2+} in the presence of various other metal cations including Zn^{2+}, Cd^{2+} and Cu^{2+} which were expected to interfere significantly. A 1 : 2 stoichiometry was found for the complex formed by **PDI-1** and Ni^{2+} by a Job's plot and by non-linear least square fitting of the fluorescence titration curves. By introducing an extra diamino ethylene group between DPA and the phenyl bridge, the receptor was modified and the high selectivity of the sensor toward Ni^{2+} shifted to Fe^{3+}. The enhancement factor of the fluorescence response of **PDI-2** to Fe^{3+} was as high as 138. The binding behavior of the receptors in these two compounds is affected significantly by the PDI fluorophores. Most interestingly, both Ni^{2+} and Fe^{3+} are paramagnetic metal ions, which are known as fluorescence quenchers and are rarely targeted with "turn-on" fluorescence probes. This result suggests that PDIs are favorable fluorophores for a "turn-on" fluorescence probe for paramagnetic transition metal ions because of their high oxidation potential.

Introduction

Fluorescent probes for sensing and monitoring chemical analytes are a topical and attractive field for chemistry, biology and environmental science due to their high sensitivity and simplicity.[1] The design and synthesis of highly effective fluorescent probes is thus a fundamental task for organic and analytical chemists. To make a useful probe, a compound must contain a "receptor", which can selectively interact with the analytes, and a "signaling site", normally a strongly emitting fluorophore.[2] Furthermore, a communication mechanism between the binding and signaling site must exist. Among the numerous mechanisms which induce signal changes upon binding of analytes, photoinduced receptor-to-fluorophore electron transfer (PET) has been widely used in the design of new sensors. A "turn-on" motif based on PET, which changes from a non-fluorescence state to a fluorescent state upon the analyte binding, was developed in the 1980s and is widely employed in many fluorophore chemosensors due to its inherently higher sensitivity as compared to the normal fluorescence quenching motif.[2a,b,3]

Perylene tetracarboxylic diimides (PDIs) have recently generated great interest in the field of photonic materials, because of their excellent thermal- and photo-stability, high luminescence efficiency, and novel optoelectronic properties.[4] PDIs are good electron acceptors with low reduction potential.[5] Therefore PDIs should be promising candidates for application as fluorophores in fluorescent probes based on PET. However, probes based on PDIs have been rarely reported so far.[6] Recently, Zhang and co-workers reported a PDI compound with photochromic spiropyranes connected at the bay positions.[6a] The fluorescence of this compound is cooperatively controlled by UV light, ferric ions and protons. Li and co-workers have developed a novel PDI compound by connecting two tridentate ligands, *i.e.* 4-[3,5-bis(2-hydroxyphenyl)-1,2,4-triazol-1-yl] benzoic acid, to the PDI core.[6b] The fluorescence of this PDI was quenched significantly upon coordination to ferric ions. Very recently, Li and co-workers have successfully grafted the PDIs onto the surface of gold nanoparticles and developed a fluorometric and colorimetric sensor for Cu^{2+}.[6d]

In the present paper, we report two PDI based probes (**PDI-1** and **PDI-2**) with "turn-on" fluorescence output. In these two probes, the PDI unit is connected to two di-(2-picolyl)-amine (DPA) groups by different bridges. The DPA groups can selectively coordinate with different metal ions. According to the literature, Zn^{2+} can be expected to coordinate particularly efficiently.[7] As long as the DPA receptor units are not involved in metal ion binding, they can act as electron donors when PDI is excited and thus quench the fluorescence of the PDI ($\Delta G = -0.26$ eV, see ESI‡ for the calculation details). The binding of metal ions at the DPA unit will block the PET between DPA and PDI and thus restore the fluorescence of PDI. To the best of our knowledge, **PDI-1** and

[a]*Department of Chemistry, Shandong University, Jinan, 250014, China. E-mail: xiyouli@sdu.edu.cn; Fax: +86-531-88564464; Tel: +86-531-88369877*
[b]*Department of Chemistry, Henan Normal University, Xinxiang, 453007, China*
[c]*Institut für Chemie und Biochemie, Freie Universität Berlin, Takustrasse 3, D-14195 Berlin, Germany. E-mail: schalley@chemie.fu-berlin.de*

† Dedicated to Professor Michael R. Wasielewski on the occasion of his 60th birthday.

‡ Electronic supplementary information (ESI) available: ^{1}H and ^{13}C NMR spectra of **PDI-1** and **PDI-2**; free energy calculation for PET from DPA to PDI; competition experiments of **PDI-1** and **PDI-2**; Stern–Volmer plot of the fluorescence quenching of **PDI-2** in the presence of excess of Fe^{3+}; fluorescence lifetime measurements for **PDI-2** in the presence of excess of Fe^{3+}; ^{1}H NMR spectra of **PDI-2** obtained during the titration with Zn^{2+} ions in DMSO-d_6; fluorescence spectra of **PDI-2** analog with excess of Fe^{3+} in DMF. See DOI: 10.1039/b921342b

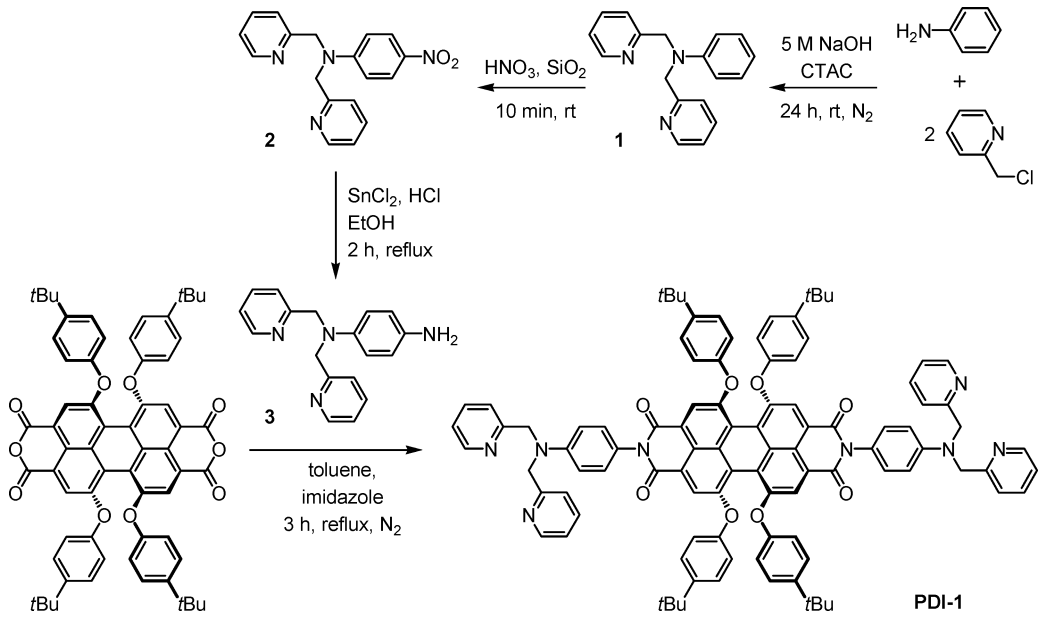

Scheme 1 Synthesis of **PDI-1**

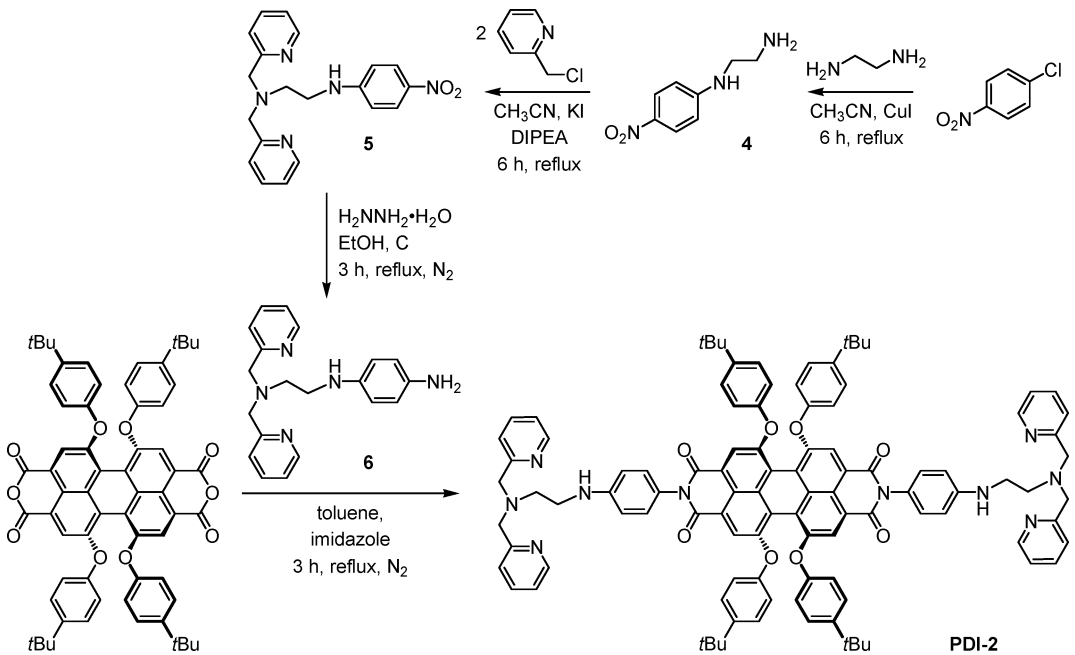

Scheme 2 Synthesis of **PDI-2**

PDI-2 (Schemes 1 and 2) represent the first examples of "turn-on" fluorescent probes based on PDI signaling units.

Results and discussion

Molecular design and synthesis

To obtain high sensitivity for a fluorescent chemosensor with "turn-on" out-put based on the PET mechanism, the background fluorescence (fluorescence of the chemosensor without analyte) must be as low in intensity as possible. Therefore the PET between the donor and acceptor must be very quick and efficient in order to maintain complete fluorescence quenching. For the given electron donor–acceptor pair, PDI–DPA, the electron transfer efficiency is determined foremost by the linker between them. For the present study, a phenyl group was chosen to connect the PDI and DPA units in our sensors, because it was earlier proven to be favorable in other systems.[7a,c,e,g,i,l,m,8]

The synthesis of **PDI-1** is depicted in Scheme 1. Compound **1** was synthesized by treatment of aniline with 2-(chloromethyl)-pyridine hydrochloride in aqueous NaOH solution with hexadecyltrimethylammonium chloride as a phase transfer catalyst with a yield of 30%. Nitration of **1** with silica supported nitric acid at room temperature in dichloromethane produces nitro derivative

2 with 71% yield. Reduction of **2** with $SnCl_2{\cdot}2H_2O$ in dilute HCl afforded **3**, which was condensed with 1,6;7,12-tetra-(4-*tert*-butylphenoxy)-perylene-3,4:9,10-tetracarboxylic dianhydride[9] in toluene with imidazole as the base to give rise to **PDI-1** in 47%. The preparation of **PDI-2** is described in Scheme 2. Compound **4** was synthesized by the condensation of 1-chloro-4-nitrobenzene with ethylene diamine in CH_3CN. Alkylation with 2-(chloromethyl)-pyridine hydrochloride afforded *N*-(4-nitrophenyl)-*N′*,*N′*-di-(2-picolyl) ethylene diamine **5**. Reduction of **5** with $NH_2NH_2{\cdot}H_2O$ over graphite powder in ethanol affords *N*-(4-amino-phenyl)-*N′*,*N′*-di-(2-picolyl) ethylene diamine **6** in 65% yield. The condensation of **6** with 1,6;7,12-tetra(4-*tert*-butylphenoxy)-perylene-3,4:9,10-tetracarboxylic dianhydride follows the procedure used for **PDI-1** and provides **PDI-2** in 87% yield. Both **PDI-1** and **PDI-2** were fully characterized by ^1H and ^{13}C NMR and MALDI-TOF mass spectra.

Absorption and fluorescence spectra of PDI-1 and PDI-2

The absorption spectra of these two PDI compounds show a strong absorption band centered around 580 nm, which is typical for PDIs with four substituents at the bay positions.[10] These results suggest that the connection of DPA groups at the imide nitrogens does not affect the ground state of PDI. This is reasonable because the frontier molecular orbital knots at the imide nitrogens block the interactions between the DPA and PDI units.[4a,5b] For the same reason, the UV–vis absorption spectra of **PDI-1** and **PDI-2** showed almost negligible changes when metal ions were present in the solution.

As expected, the fluorescence from the PDI fluorophore in both **PDI-1** and **PDI-2** was completely quenched, indicating that the electron transfer from DPA to PDI in both **PDI-1** and **PDI-2** is quick and efficient. Usually, the fluorescence lifetime for the PDI with four *p*-*t*-butylphenoxyl groups connected at the bay positions is around 6 ns as reported in the literature.[9,11] The fluorescence lifetime of **PDI-1** and **PDI-2** cannot be determined by an instrument with a 0.05 ns time limitation, which means that the lifetimes in **PDI-1** and **PDI-2** are shorter than 50 ps and the electron transfer rate constant from DPA to PDI is larger than 1.86×10^{10} s^{-1}.

Fluorescence response of PDI-1 to different metal cations

The PDI fluorescence was restored in the presence of different metal ions. Fig. 1 shows the corresponding fluorescence spectra of **PDI-1** in DMF (6 μM) after addition of different metal ions (8 equiv.). The emission peak appears at about 609 nm, which is the typical emission of PDI without any significant peak shift. This result suggests no other interaction between the DPA and the PDI unit exists in the excited state besides the efficient electron transfer between both units in the absence of metal coordination. As shown in Fig. 1, the most distinctive fluorescence intensity enhancement resulted when Ni^{2+} was added. Addition of Co^{2+} and Zn^{2+} enhanced the fluorescence intensity of **PDI-1** too, but by an obviously much smaller magnitude. The presence of Cd^{2+} and other metal ions resulted in negligible fluorescence intensity changes under identical experimental conditions.

The fluorescence intensity enhancements are usually described by the enhancement factor (EF), which is calculated from the

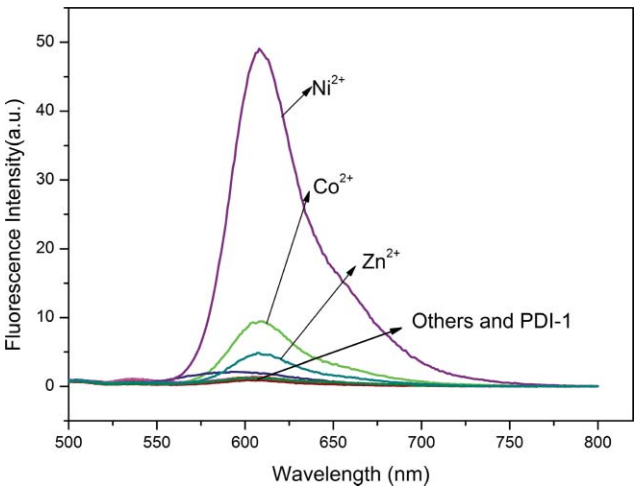

Fig. 1 Fluorescence spectra of **PDI-1** in the presence of different metal ions Na^+, Cr^{3+}, Mn^{2+}, Fe^{3+}, Fe^{2+}, Co^{2+}, Ni^{2+}, Cu^{2+}, Zn^{2+}, Cd^{2+}, Hg^{2+} and Pb^{2+} in DMF solutions. $\lambda_{ex} = 440$ nm, [**PDI-1**] $= 6.0 \times 10^{-6}$ M, $[M^{n+}] = 4.8 \times 10^{-5}$ M (8 equiv.).

fluorescence intensities of the chemosensor with (F) or without metal ions (F_0). Fig. 2 compares the EFs of various metal ions (14 equiv.) towards the fluorescence of **PDI-1** in DMF. In the absence of metal ions, the fluorescence of **PDI-1** was strongly quenched by the PET process with a fluorescence quantum yield (Φ) as small as ~0.0003. But in the presence of Ni^{2+}, the fluorescent intensity of **PDI-1** increased by over 49-fold, with Φ increased to 0.016. The EFs of Co^{2+}, Zn^{2+} and Cd^{2+} calculated following the same method were 8 ($\Phi = 0.0025$), 6 ($\Phi = 0.0019$) and 1 ($\Phi =$ ~0.0004), respectively. **PDI-1** thus shows "turn-on" fluorescence, and displays a quite remarkably high selectivity for Ni^{2+} among the various ions under study.

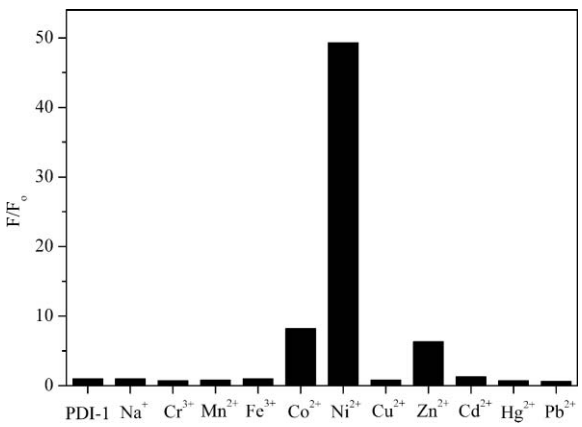

Fig. 2 Fluorescence responses of **PDI-1** (8 μM) to various metal cations (14 equiv.) in DMF ($\lambda_{ex} = 440$ nm).

The selective response of **PDI-1** towards Ni^{2+} is also reflected by the fluorescence lifetimes of the different fluorescent **PDI-1**–metal complexes: Ni^{2+}: 0.33 ns; Co^{2+}: 0.25 ns; Zn^{2+}: 0.17 ns. The fluorescence lifetimes of other metal complexes of **PDI-1** are too short to be measured accurately. However, the fluorescence lifetime of a standard PDI with tetraphenoxyl groups connected at the bay positions and hexyl groups at the imide nitrogen atoms is measured to be 5.46 ns under identical conditions. The

significantly shorter fluorescence lifetimes of the metal complexes of **PDI-1** suggest a contribution from an additional non-radiative decay process in the metal complexes, such as the incompletely hindered electron transfer from DPA to PDI or simply a heavy atom effect. Consequently, the different fluorescence lifetimes of the metal complexes provide another complementary means to discriminate Ni^{2+} from other transition metal ions.

The high selectivity of **PDI-1** for Ni^{2+} is surprising because the DPA chelating groups are expected to exhibit high affinity towards Zn^{2+}, Cd^{2+} or Cu^{2+}, but small affinity towards other metal cations as suggested by earlier reports.[7] Moreover, metal ions with open shell d-orbitals such as Ni^{2+}, Cu^{2+} and Fe^{3+} frequently act as quenchers to the fluorescence of fluorophores *via* electron or energy transfer between metal ion and fluorophore.[12] In contrast, closed d-shell transition metal ions such as Zn^{2+} and Cd^{2+} usually do not quench the fluorescence.

The high stability of the coordination compound of DPA with Ni^{2+} or Cu^{2+} is well known in the literature.[13] However, in earlier studies the binding properties of DPA with metal ions varied according to the fluorophores and the linkers, as well as the experimental conditions. In most cases, DPA has been shown to have good affinity for Zn^{2+} and, consequently, was previously used in zinc-selective sensors.[7a,b,d-j,l-q] In some cases, DPA showed good selectivity toward Cd^{2+} in a biological environment,[7c] but it is not known to show high selectivity towards Ni^{2+} over Cd^{2+}, and Zn^{2+}. This must be related to the electron transfer mechanism in **PDI-1**. The electron donor in **PDI-1** is the nitrogen atom connected directly to the phenyl linker. When this nitrogen atom coordinates to metal ions, its electron donating ability is reduced and thus the electron transfer from the nitrogen atom to the PDI π-system is hindered and the fluorescence restored. Although plenty of examples suggested that DPA forms stable complexes with Zn^{2+}, crystal structures of these complexes revealed that the aniline nitrogen atom does not always participate in the coordination.[14a,b] Thus, even when **PDI-1** coordinates to Zn^{2+}, the aniline nitrogen atom might be still available for fluorescence quenching. In contrast, crystal structures of Ni^{2+} complexes of different DPAs revealed this nitrogen atom to be always coordinated to the nickel cation.[14a,15] Therefore the coordination of Ni^{2+} induces significant enhancement of fluorescence.

ESI mass spectrometry of PDI-1 metal complexes

The higher stability of the Ni^{2+} complex of **PDI-1** over that of Zn^{2+} and other metal ions could qualitatively be confirmed by the ESI mass spectra obtained from competition experiments. In these experiments, **PDI-1** was mixed with 4 equiv. of two different metal salts in DMF. The solution was afterwards used to record ESI mass spectra. Fig. 3 shows the results. The first spectrum serves as a reference. When 4 equiv. $NiCl_2$ are mixed with **PDI-1**, the major signal in the spectrum corresponds to a doubly charged [**PDI-1**·$(NiCl)_2$]$^{2+}$ complex at m/z 858. As expected, the stoichiometry of the complex is 1 : 2 and both coordination sites are occupied by a Ni^{2+} ion, of which three binding sites are occupied by the DPA ligand. The fourth ligand is the chloride counterion. Not unexpectedly, the doubly charged Ni^{2+} complex is the dominating signal for a mixture of nickel and sodium chloride (Fig. 3b); no signal is observed for sodium coordination. When $FeCl_3$ is used as the competitor, one might have expected to find either a

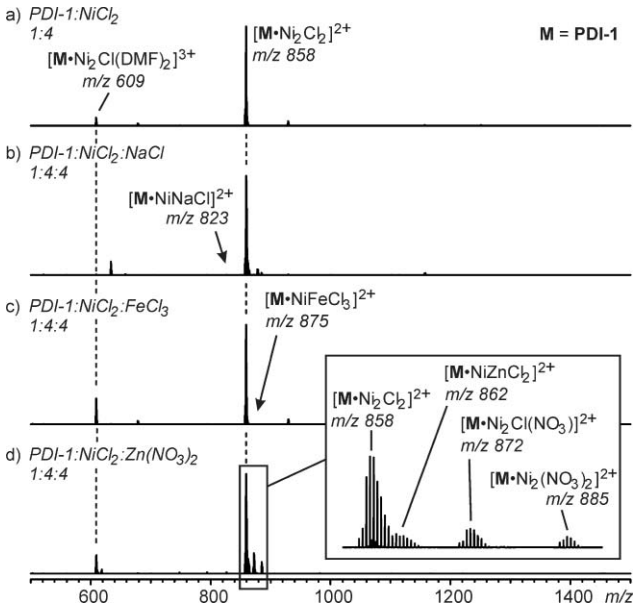

Fig. 3 ESI mass spectra of 8 μM DMF solutions of **PDI-1** with (a) 4 equiv. of $NiCl_2$, (b) 4 equiv. of both $NiCl_2$ and NaCl, (c) 4 equiv. of both $NiCl_2$ and $FeCl_3$, and (d) 4 equiv. of both $NiCl_2$ and $Zn(NO_3)_2$.

[**PDI-1**·(NiCl)$(FeCl_2)$]$^{2+}$ complex or a [**PDI-1**·$(FeCl_2)_2$]$^{2+}$ complex. However, this is not the case. Ni^{2+} obviously binds more strongly. Finally, when $ZnCl_2$ is added as the second transition metal salt, a mixed-metal [**PDI-1**·(NiCl)(ZnCl)]$^{2+}$ ion is observed with low intensity. The two isotope patterns of this ion and the nickel homodimer overlap. In addition, signals for anion exchanges are observed, because two different counterions were used in this experiment. Still, the nickel complex is by far the most abundant species appearing in this mass spectrum and thus these MS results nicely confirm the analysis of the fluorescence experiments described above.

Fluorescence titration and competition experiments

To get further insight into the stoichiometry and the stability of the **PDI-1**–Ni^{2+} complexes, a Job plot and fluorescence titration experiments were performed at room temperature in DMF, Fig. 4a. The 1 : 2 binding mode between **PDI-1** and Ni^{2+} as observed by mass spectrometry was also clearly supported by the data of Job's plot. A plot of F *versus* $X_{[Ni^{2+}]}$ ([Ni^{2+}]/([Ni^{2+}]+[**PDI-1**])) showed that the F value arrived at its maximum at a molar fraction of *ca.* 0.68, Fig. 4a confirming the 1 : 2 binding stoichiometry.

Based on the 1 : 2 stoichiometry, the Benesi–Hildebrand equation can be used to evaluate the binding strength:[16]

$$\frac{1}{F - F_{min}} = \frac{1}{K_a \cdot (F_{max} - F_{min}) \cdot [Ni^{2+}]^2} + \frac{1}{F_{max} - F_{min}}$$

F_{min} and F are the fluorescence intensity of **PDI-1** in the absence and presence of Ni^{2+}, respectively. F_{max} is the fluorescence intensity obtained with a large excess of Ni^{2+}, K_a the association constant of the Ni^{2+} complex of **PDI-1**, and [Ni^{2+}] was the concentration of Ni^{2+}. As shown in Fig. 4b and c, the plot of $1/(F - F_{min})$ against $1/[Ni^{2+}]^2$ is linear. From the Benesi–Hildebrand analysis,

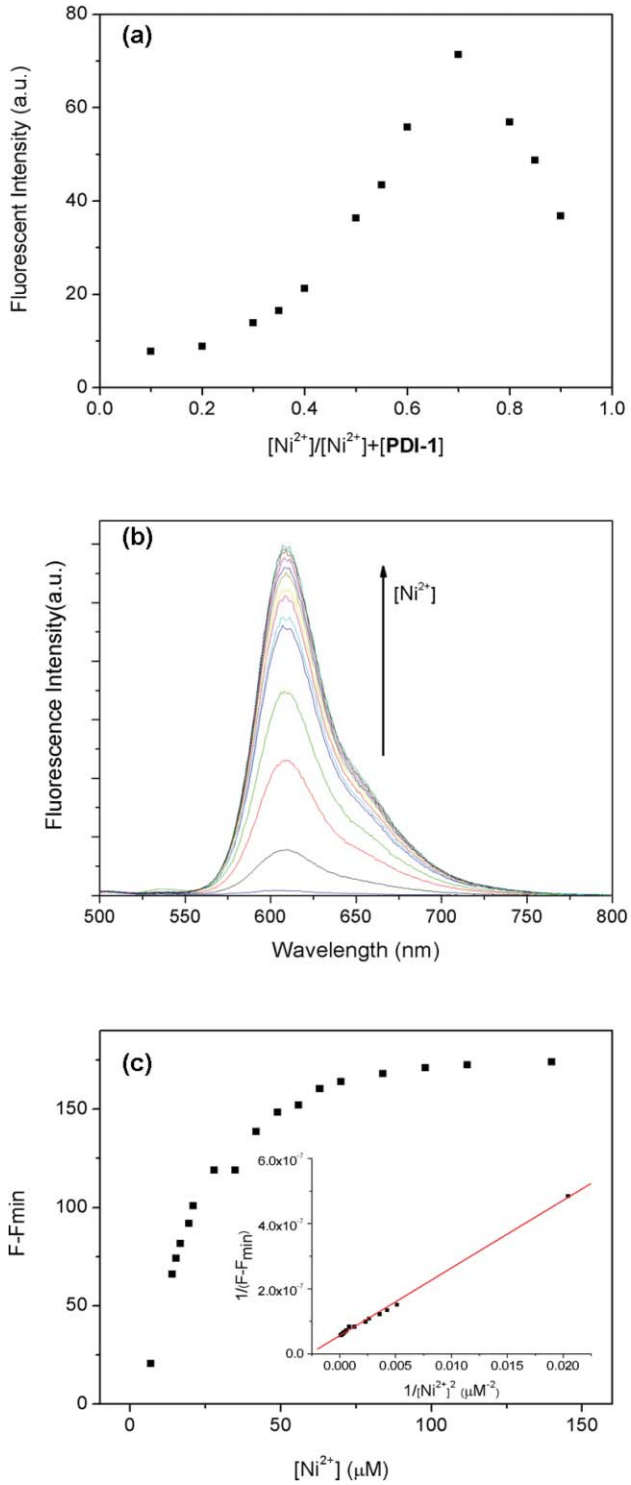

Fig. 4 (a) Job's plot for determining the stoichiometry of **PDI-1** and Ni^{2+} in DMF, where the integrated fluorescence was plotted against the mole fraction of Ni^{2+} ([Ni^{2+}]/([Ni^{2+}]+[**PDI-1**])). (b) Fluorescence titration spectra of **PDI-1** (7 μM) upon increasing the concentration of Ni^{2+} in DMF. The excitation wavelength was 440 nm. (c) Relative fluorescence intensities ($F - F_{min}$) as a function of the concentration of Ni^{2+} in DMF. The inset shows the Benesi–Hildebrand plot of $1/(F - F_{min})$ against $1/[Ni^{2+}]^2$.

the association constant K_a is determined to be 2.7×10^9 M^{-2}, thus confirming the high nickel affinity of **PDI-1**.

Competition experiments were also conducted by recording fluorescence spectra of 8 μM DMF solutions of **PDI-1** with Ni^{2+} (4 equiv.) and Na^+, Cr^{3+}, Mn^{2+}, Fe^{3+}, Co^{2+}, Cu^{2+}, Zn^{2+}, Cd^{2+}, Hg^{2+}, or Pb^{2+}(12 equiv.) ions (Figure S5, in the ESI‡). Na^+, Cr^{3+}, Mn^{2+}, Fe^{3+}, Co^{2+} ions did not interfere significantly with the fluorescence of the **PDI-1**–Ni^{2+} complex; Co^{2+},Cu^{2+}, Zn^{2+}, Cd^{2+}, Hg^{2+}, and Pb^{2+} induced slight fluorescence quenching, although they were present in 3-fold excess as compared to the Ni^{2+} concentration. These results confirm the ability of **PDI-1** to sense Ni^{2+} with high selectivity even in the presence of other metal ions.

Paramagnetic metal ions, such as Fe^{3+}, Cu^{2+} and Ni^{2+}, usually induce significant fluorescence quenching *via* electron transfer or energy transfer from the fluorophore to the metal complexes. As one of the important quenching mechanisms, the redox interaction, *i.e* the electron transfer between the fluorophore and metal ions, can be efficiently reduced by simply increasing the electron affinity of the fluorophore.[17] PDI is hard to oxidize so the electron transfer from the excited state to the metal ion is difficult. One may argue that the hindered electron transfer between **PDI-1** and Ni^{2+} might also be attributed to the virtual decoupling between the PDI fluorophore and the terminal receptors DPA because of the almost perpendicular arrangement of the PDI plane relative to the plane of the phenyl bridge, rendering electron transfer from the PDI excited state to Ni^{2+} unfavorable as described in literature.[18] It is worth noting that only one example, which had a fluorescence enhancement output in the presence of Ni^{2+}, has been reported so far in the literature.[19] But it cannot distinguish Ni^{2+} from Cu^{2+} and Zn^{2+} due to the less selective binding of the cryptate to the transition metal ions. To the best of our knowledge, **PDI-1** represents the first example of a fluorescent probe for Ni^{2+} with "turn-on" output that can distinguish Ni^{2+} from Zn^{2+}, Cu^{2+}, Fe^{3+} and other transition metal ions.

Metal-sensing properties of PDI-2

The response of **PDI-2** to the presence of various transition metal ions is different from that of **PDI-1** (Fig. 5). The fluorescence intensity enhanced significantly in the presence of Fe^{3+} while only

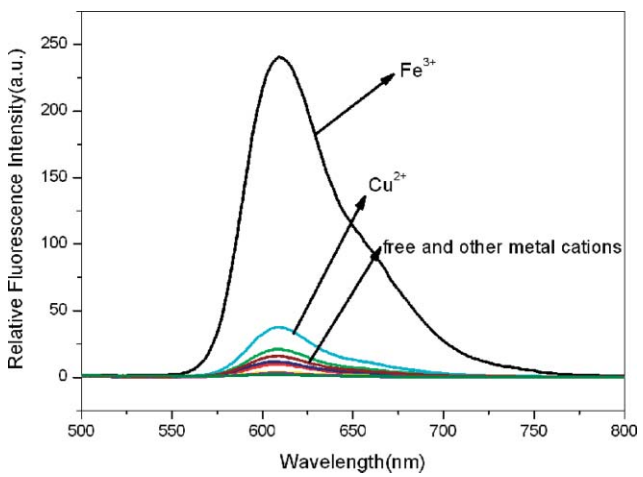

Fig. 5 Fluorescence spectra of **PDI-2** in the presence of different metal ions including Na^+, Cr^{3+}, Mn^{2+}, Fe^{3+}, Co^{2+}, Ni^{2+}, Cu^{2+}, Zn^{2+}, Cd^{2+}, Hg^{2+} and Pb^{2+} in DMF solutions (λ_{ex} = 440 nm, [**PDI-2**] = 5 μM, [M^{n+}] = 20 μM, (4 equiv.)).

a slight increase in the fluorescence intensity was observed in the presence of Co^{2+}, Zn^{2+} and Cu^{2+}. Other metal ions resulted in negligible changes of the fluorescence spectra as compared to free **PDI-2**. The EFs of **PDI-2** in the presence of different metal ions are compared in Fig. 6. The largest EF is that of Fe^{3+}, which amounts to 138, since the fluorescence quantum yield, Φ, increased from ~0.0004 to 0.04. The EFs of Cu^{2+}, Co^{2+}, and Zn^{2+} are 18 ($\Phi = 0.0076$), 10 ($\Phi = 0.0038$) and 7 ($\Phi = 0.0034$), respectively. This result suggests that **PDI-2** afforded remarkable "turn-on" fluorescence, and showed high selectivity towards Fe^{3+} among the various ions being investigated, including Zn^{2+} for which again a significant increase would have been expected.

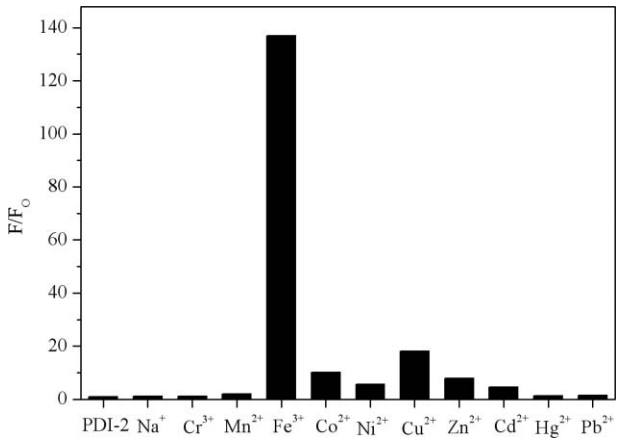

Fig. 6 Fluorescence response of **PDI-2** (5 μM) to various metal cations (4 equiv.) in DMF. Bars represent EF (enhancement factor F/F_o), λ_{ex} = 440 nm.

The high selectively of **PDI-2** towards Fe^{3+} was further confirmed by the competition experiment (Figure S6 in the ESI‡). When the mixed solution of Fe^{3+} (4 equiv.) with Na^+, Cr^{3+}, Mn^{2+}, Co^{2+}, Ni^{2+}, Cu^{2+}, Zn^{2+}, Cd^{2+}, Hg^{2+}, or Pb^{2+}(8 equiv.) was added to the solution of **PDI-2** (5 μM), the Na^+, Cr^{3+}, Mn^{2+}, Cd^{2+} ions showed no disturbance to the fluorescence of **PDI-2**; Co^{2+}, Ni^{2+}, Hg^{2+}, Pb^{2+}, Cu^{2+} and Zn^{2+} induced small fluorescence quenching. Therefore, these tested metal cations had no significant interference to the sensing by **PDI-2** of iron(III) ions, and **PDI-2** exhibited high selectivity towards Fe^{3+} while coexisting with other metal ions.

In **PDI-2**, the DPA group was connected to the phenyl group by an ethylene diamine bridge, which represents another popular ionophore, *N*-ethyldipicolylamine aniline (EDPA). The ethylene diamine linker provides an additional nitrogen atom for coordination to the metal ions. EDPA has been employed widely in various fluorescence sensors with different fluorophores based on PET.[7b,e,g,i,n] These sensors show exclusively high selectivity towards Zn^{2+}. The high selectivity of **PDI-2** towards Fe^{3+} over Zn^{2+} is thus unexpected. Furthermore, the structural change from DPA to EDPA changes the binding behavior of our PDI sensors significantly by shifting the selectivity from Ni^{2+} to Fe^{3+}. The ^{1}H NMR spectra of **PDI-2** in the absence and presence of 2 equivalents of Zn^{2+} in DMSO-d_6 were recorded (Fig. 7). The significant shifts of the EDPA signals relative to those observed in the absence of Zn^{2+} suggest the efficient coordination of EDPA with Zn^{2+}. However, the signals of the protons on the phenyl

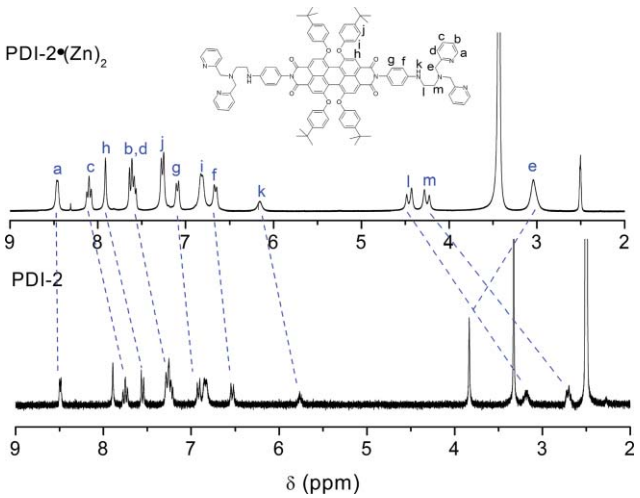

Fig. 7 ^{1}H NMR spectra of **PDI-2** and **PDI-2**·Zn^{2+} in DMSO-d_6.

linkage do not change much, which indicates that the aniline nitrogen atoms do not participate in the coordination. The efficient binding of the **PDI-2** with Zn^{2+} was further confirmed by the ^{1}H NMR titration experiment as shown in Figure S10 (see the ESI‡). We do not find a gradual shift of the signal positions, but instead see some new peaks after the addition of Zn^{2+}. This suggests that the complex between **PDI-2** and Zn^{2+} is very stable. This is also supported by the fact that the ^{1}H NMR spectra of **PDI-2** change dramatically when the mole ratio (Zn^{2+}/**PDI-2**) is in the range of 0.5–2, but do not change any further after the mole ratio is in excess of 2. On the one hand this verified the 1 : 2 stoichiometry for the **PDI-2**–Zn^{2+} complex, as well as on the other hand indicating that the complex between **PDI-2** and Zn^{2+} has very high stability This has proved that **PDI-2** can bind to Zn^{2+} with high stability. However, because the electron donor, the amino group connected directly at the phenyl ring, does not participate in the coordination, the presence of Zn^{2+} does not restore the fluorescence of **PDI-2**. We cannot record the ^{1}H NMR spectrum of **PDI-2** in the presence of Fe^{3+} because of the paramagnetic nature of the complex. Therefore, we do not know how the Fe^{3+} ions coordinate with the receptor EPDA at this stage, but the ESI mass spectra of the 1 : 2 mixture of **PDI-2** and $FeCl_3$ show clearly one peak, which corresponds to a complex with a 1 : 2 stoichiometry, [(**PDI-2**)($Fe_2O(Cl_2)$)]$^{2+}$ (Fig. 8). This result indicates that the complex formed between **PDI-2** and $FeCl_3$ again has a 1 : 2 stoichiometry.

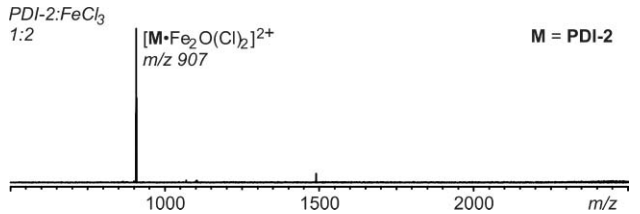

Fig. 8 ESI mass spectrum of a 1 : 2 mixture of **PDI-2** and $FeCl_3 \cdot 6H_2O$ in DMF. (The only major signal corresponds to a 2 : 1 iron complex of **PDI-2** whose charges are counterbalanced by one oxo and two chloride anions. While the source of the oxo ligand is likely the water from the metal salt, it is not fully clear why no other combinations of counterions are observed.)

The fluorescence enhancements of **PDI-2** in the presence of Fe^{3+} at different concentrations are shown in Fig. 9. With the increase

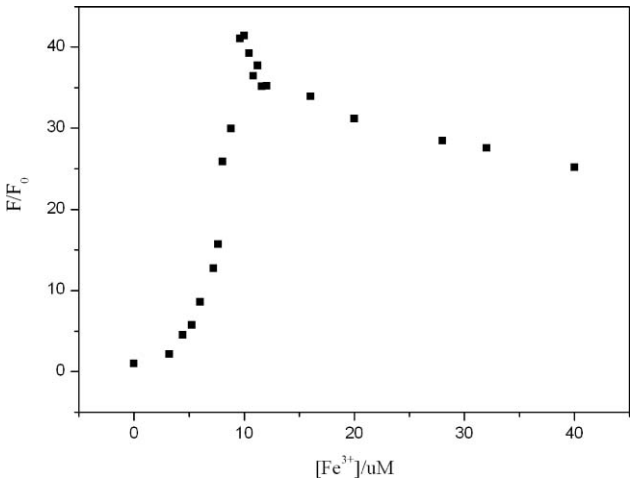

Fig. 9 Relative fluorescence intensities (F/F_o) of **PDI-2** (3 μM) as a function of the concentration of Fe^{3+} in DMF.

of the concentration of Fe^{3+}, the fluorescence intensities of **PDI-2** increase significantly at the early stage (<3 equivalents), but decrease again after the concentration of Fe^{3+} exceeds this ratio. A similar phenomenon has earlier been found for a rhodamine based Cu^{2+} sensor and was attributed to the formation of H aggregates of the metal complexes with different stoichiometry.[20] But in our case, no significant changes in the absorption spectra were observed. We ascribe this fluorescence quenching in the presence of excess Fe^{3+} to the dynamic quenching of free Fe^{3+} to the fluorescent [(**PDI-2**)($Fe_2O(Cl_2)$)]$^{2+}$ based on the following two reasons. The first is the Stern–Volmer plot (I_0/I *vs.* [Fe^{3+}], see the ESI‡, Figure S7) in the concentration range of [Fe^{3+}] > 4[**PDI-2**], which gives a linear relationship between I_0/I and [Fe^{3+}] and suggests no interactions between the fluorescent [(**PDI-2**)($Fe_2O(Cl_2)$)]$^{2+}$ and quencher Fe^{3+}. The second reason is that the lifetimes of [(**PDI-2**)($Fe_2O(Cl_2)$)]$^{2+}$ in the presence of excess Fe^{3+} show mono-exponential decay (see the ESI‡ Figures S8–S9). This result suggests that [(**PDI-2**)($Fe_2O(Cl_2)$)]$^{2+}$ is the only fluorescent component and excludes the presence of new fluorescent species in the presence of excess Fe^{3+}. Both the Stern–Volmer plot and the fluorescence lifetime measurements reveal that the excess Fe^{3+} does not induce new fluorescent species in the reaction mixture. Therefore, the quenching caused by excess Fe^{3+} might be induced simply by the dynamic collision between Fe^{3+} and [(**PDI-2**)($Fe_2O(Cl_2)$)]$^{2+}$. To verify this hypothesis, the fluorescence titration experiment was conducted with a PDI analog, *N*,*N*′-di-*n*-butyl-1,6,7,12-tetra(4-***tert***-butylphenoxy)perylene-3,4:9,10-tetracarboxylic diimide, which does not have metal binding sites. The dynamic fluorescence quenching was assuredly observed with the increasing of the concentration of Fe^{3+} in DMF (Figure S11 in the ESI‡). This result indicates that the suggested dynamic fluorescence quenching mechanism for the **PDI-2**–Fe^{3+} complex by excess of Fe^{3+} is reasonable.

Because of the drop in the fluorescence intensity after the maximum at [Fe^{3+}] = 3 equivalents of **PDI-2**, the fitting of the titration curve following the Benesi–Hildebrand equation does not give any reliable results. Therefore the stoichiometry as well as the association constant can neither be determined quantitatively by the fluorescence titration nor by a Job's plot.

Paramagnetic Fe^{3+} is a well-known efficient fluorescence quencher like Ni^{2+}. Consequently, developing novel probes for Fe^{3+} with fluorescence enhancement is still a challenging task. Up to now, molecular probes that selectively show amplified fluorescence in the presence of Fe^{3+} are still rare. Only a few examples have been reported in the literature.[21] For instance, the probes based on receptor 1-oxa-4,10-dithia-7-aza macro cycle developed by Bricks and co-workers show high selectivity towards Fe(III) with turn-on output in methanol.[21a] Some rhodamine-based spirolactam probes exhibit significant fluorescence enhancement in the presence of Fe^{3+} because of the exchange between spirocyclic and ring-open forms.[21b-d] Brückner and colleagues developed a squarate hydroxamate-coumarin-based chemosensor for Fe^{3+} with turn-on output based on oxidation reactions.[21e] Recently, a phenanthroimidazole-based probe developed by Lin and co-workers showed ratiometric fluorescence response to Fe^{3+}.[21f] **PDI-2** represents another example of the small collection of Fe^{3+} probes with turn-on fluorescence output.

Conclusion

In summary, two novel "turn-on" fluorescent probes bearing PDI as the fluorophore were successfully prepared and their sensing capabilities for transition metal ions were examined. **PDI-1** exhibited high selectivity for Ni^{2+} in the presence of various metal cations including Zn^{2+}, Cd^{2+} and Cu^{2+} which were expected to interfere. A 1 : 2 stoichiometry was obtained from mass spectrometry as well as a Job's plot and non-linear fitting of the fluorescence titration curves. To the best of our knowledge, this is the first example of a fluorescent probe for Ni^{2+} that demonstrated significant fluorescent enhancement. **PDI-2** presented high selectivity toward Fe^{3+} with a fluorescence enhancement factor as high as 138. Most interestingly, both Ni^{2+} and Fe^{3+} are paramagnetic metal ions, which are normally known as fluorescence quenchers. Thus, it is challenging to develop "turn-on" fluorescent probes for them. The result of our research suggests that PDIs are favorable fluorophores for "turn-on" fluorescence probes for paramagnetic transition metal ions. Considering the multitude of choices for the structure modification of PDI, we are confident that the design strategy presented here will help to develop a new class of excellent PDI-based chemosensors with practical application in many sensing fields, such as environmental research and biology.

Experimental section

General methods

^1H and ^{13}C NMR spectra were recorded on a Bruker 400 MHz NMR spectrometer with chemical shifts reported in ppm (in $CDCl_3$, TMS as internal standard). MALDI-TOF mass spectra were taken on a Bruker/ultraflexinstrument. ESI mass spectra were recorded on a Varian/Ionspec QFT-7 Fourier-transform ion-cyclotron-resonance (FT-ICR) mass spectrometer with a Micromass *Z*-spray ESI ion source. Absorption spectra were measured on HITACHI U-4100 spectrophotometer. Fluorescence emission spectra and fluorescence lifetime were measured on an ISS K2 system. IR spectra were recorded on a Nicolet Impact 400D infrared spectrophotometer.

Fluorescent response experiments

Stock solutions (1 mM) of each metal salt, **PDI-1** and **PDI-2** (0.1 mM) in DMF were prepared. Test solutions were prepared by placing 0.3–1 ml of the probe's stock solution into a test tube, adding an appropriate aliquot of each metal stock solution, and then diluting the solution to 10 ml with DMF to give the final concentration. After complete mixing, measurements of UV–vis absorption and fluorescent emission were carried out on above mentioned spectrophotometers with a 1 cm standard quartz cell.

Materials

The salts used in stock solutions of metal ions were NaCl, $CrCl_3·6H_2O$, $MnCl_2·4H_2O$, $FeCl_3·6H_2O$, $CoCl_2·6H_2O$, $NiCl_2·6H_2O$, $Cu(OAc)_2·H_2O$, $Zn(NO_3)_2·6H_2O$, $CdCl_2·2.5H_2O$, $Hg(NO_3)_2$, $Pb(NO_3)_2$. 1,6,7,12-Tetra(4-*tert*-butylphenoxy)-perylene-3,4:9,10- tetracarboxylic dianhydride,[22] compounds **1**,[7e] **4**[23] and **5**[23] were synthesized according to literature methods. Other chemicals were purchased from commercial sources. Solvents were of analytical grade and purified by standard methods.

4-Nitro-*N*,*N*-di-(2-pyridylmethyl)-aniline (2). To the HNO_3 solution (100 ml, 65%), SiO_2 (30 g, 200-300 mesh) was rapidly added with vigorous stirring at room temperature over 5 min. After stirring at room temperature for 3 days, the nitrated dry SiO_2 was obtained. To a stirred suspension of the nitrated SiO_2 (7 g) in CH_2Cl_2 (200 ml), compound **1** (1.7 g, 6.18 mmol) was added. After being stirred vigorously at room temperature for 10 min, a dark-green suspension formed, which was further neutralized to pH 7.5–8 with triethylamine (TEA). The resulting brownish suspension was stirred for another 10 min, after which the SiO_2 was filtered and washed several times with CH_2Cl_2. After evaporation of the solvent on a rotary evaporator, compound **2** (1.4 g, 4.38 mmol) was obtained as yellow oil in 71% yield through column chromatography (silica 200–300 mesh, CH_2Cl_2–CH_3OH 100/2, v/v); ^{1}H NMR (400 MHz, $CDCl_3$, 25 °C, TMS): $\delta = 8.58$ (d, 2H), 8.00 (d, 2H), 7.66 (tri, 2H; pyridyl), 7.24 (d, 2H), 7.19 (tri, 2H; pyridyl), 6.75 (d, 2H), 4.94 (s, 4H; NCH_2); MS (ESI): *m*/*z*: 321.36 [M+H$^+$]; Calcd for $C_{18}H_{16}N_4O_2$: 320.35.

4-Amino-*N*,*N*-di-(2-pyridylmethyl)-aniline (3)[24]. To a solution of **2** (2.23 g, 6.96 mmol) in ethanol (100 ml), a mixture of concentrated HCl (50 ml) and $SnCl_2·2H_2O$ (9.5 g, 42 mmol) was added at room temperature. The resulting yellow solution was refluxed for 24 h. After being cooled to room temperature and diluted with H_2O, the resulting mixture was carefully alkalized to pH 7.5–8 with a 30% NH_4OH aqueous solution. A white suspension formed in the reaction mixture. The reaction mixture was extracted with ethyl acetate, and the combined organic phases were dried over anhydrous $MgSO_4$ overnight. After evaporation of the solvent, compound **3** (0.82 g, 2.83 mmol) was obtained as white solid in 41% yield *via* column chromatography (silica 200–300 mesh, CH_2Cl_2–CH_3OH 100/5, v/v); ^{1}H NMR (400 MHz, $CDCl_3$, 25 °C, TMS): $\delta = 8.55$ (d, 2H), 7.58 (tri, 2H), 7.28 (d, 2H), 7.12 (t, 2H), 6.58–6.50 (m, 4H), 4.72 (s, 4H; NCH_2), 3.37 (s, 2H; NH_2); MS (ESI): *m*/*z*: 291.17 [M+H$^+$]; Calcd for $C_{18}H_{18}N_4$: 290.37.

***N*,*N*′-Bis-(*N*,*N*-di-(2-pyridylmethyl)-aniline)-1,6,7,12-tetra-(4-*tert*-butylphenoxy)-perylene-3,4:9,10-tetracarboxylic-diimide (PDI-1).** A mixture of 1,6:7,12-tetra(4-*tert*-butylphenoxy)-perylene-3,4:9,10-tetracarboxylic dianhydride (820 mg, 0.83 mmol), compound **3** (830 mg, 2.86 mmol) and imidazole (3.00 g, 44.05 mmol) in toluene (100 mL) was refluxed under N_2 for 3 h. After the solvent was evaporated, the residue was dissolved in chloroform and washed with water to remove the imidazole. The collected organic phase was dried over anhydrous $MgSO_4$ for overnight. After evaporation of the chloroform, the crude product was purified by column chromatography on silica gel (200–300 mesh) using 100 : 3 (v/v) $CHCl_3$–MeOH as the eluent. A subsequent recrystallization from a mixture of $CHCl_3$ and MeOH gave pure product. **PDI-1** was collected as a dark purplish solid (598.6 mg, 0.391 mmol, 47%); ^{1}H NMR (400 MHz, $CDCl_3$, 25 °C, TMS): $\delta = 8.58$ (d, 4H; pyridyl), 8.20 (s, 4H; perylene), 7.64 (tri, 4H; pyridyl), 7.30 (d, 4H; pyridyl), 7.22 (d, 8H; phenyl), 7.15 (tri, 4H; pyridyl), 7.01 (d, 4H; phenyl), 6.84 (d, 8H; phenyl), 6.78 (d, 4H; phenyl), 4.85 (s, 8H; NCH_2), 1.26 (s, 36H; $C(CH_3)_3$); ^{13}C NMR (400 MHz, $CDCl_3$, 25 °C, TMS): $\delta =$ 163.9, 156.4, 156.0, 152.9, 149.7, 148.2, 147.3, 136.9, 133.1, 129.0, 126.6, 124.5, 122.7, 122.1, 120.9, 120.6, 120.2, 119.7, 119.3, 112.9, 57.4, 34.3, 31.4; MS (MALDI-TOF): *m*/*z*: 1529.8 [M$^+$]; Calcd for $C_{100}H_{88}N_8O_8$ (*m*/*z*): 1529.8; IR (KBr) [cm^{-1}] 2958 (C–H), 2866 (C–H), 1707 (C=O), 1671 (C=O), 1589 (C=C, perylene ring).

***N*-(4-Amino-phenyl)-*N*′,*N*′-[di-(2-pyridylmethyl)]-ethylenediamine (6)[25].** Compound **5** (2.62 g, 7.22 mmol), $NH_2NH_2·H_2O$ (85%, 10 ml), and graphite (6 g) were heated in refluxing EtOH (150 mL) for 24 h under N_2 protection. After being cooled to room temperature, the reaction mixture was diluted with CH_2Cl_2 (150 mL). Graphite was separated from the reaction mixture by filtration. After evaporation of the solvent, compound **6** (1.56 g, 4.70 mmol) was collected as light brown oil in 65% yield *via* column chromatography (silica 200–300mesh, CH_2Cl_2–CH_3OH 100/6, v/v). ^{1}H NMR (300 MHz, $CDCl_3$, 25 °C, TMS): $\delta = 8.54$ (d, 2H), 7.65 (tri, 2H), 7.59 (d, 2H), 7.13 (tri, 2H), 6.60 (d, 2H), 6.52 (d, 2H), 3.87 (s, 4H; NCH_2C), 3.48 (br, 2H, NH_2), 3.13 (tri, 2H), 2.87 (tri, 2H).

***N*,*N*′-Bis-(*N*″-2-(*N*‴,*N*‴-di-(2-pyridylmethyl)-amino-ethylene)-aniline)-1,6,7,12-tetra-(4-*tert*-butylphenoxy)-perylene-3,4:9,10-tetracarboxylic-diimide (PDI-2).** A mixture of 1,6:7,12-tetra-(4-*tert*-butylphenoxy)-perylene-3,4:9,10-tetracarboxylic dianhydride (800 mg, 0.825 mmol), compound **6** (1.24 g, 3.72 mmol), imidazole (3.00 g, 44.05 mmol) and toluene (120 mL) was refluxed under N_2 for 3 h. After the solvent was evaporated under reduced pressure, the residue was dissolved in chloroform and washed with water to remove the imidazole. The collected organic phase was dried over anhydrous $MgSO_4$ and evaporated to dryness. By recrystallization from a mixture of $CHCl_3$ and MeOH, excess compound **6** was removed. After a second recrystallization from a mixture of $CHCl_3$ and *n*-hexane, the pure product was obtained. **PDI-2** was collected as a purplish-red solid (1.16 g, 0.716 mmol, 87%). ^{1}H NMR (400 MHz, $CDCl_3$, 25 °C, TMS): $\delta = 8.55$ (d, 4H; pyridyl), 8.23 (s, 4H; perylene), 7.62 (tri, 4H; pyridyl), 7.43 (d, 4H; pyridyl), 7.21 (d, 8H; phenyl), 7.14 (tri, 4H; pyridyl), 6.97 (d, 4H; phenyl), 6.86 (d, 8H; phenyl), 6.64 (d, 4H; phenyl), 3.90 (s, 8H; NCH_2C), 3.18 (tri, 4H; $NHCH_2$), 2.90 (tri, 4H; $NHCH_2CH_2$), 1.26 (s, 36H; $C(CH_3)_3$); ^{13}C NMR (400 MHz, $CDCl_3$, 25 °C, TMS):

δ = 163.9, 159.1, 156.0, 152.9, 149.1, 148.7, 147.3, 136.5, 133.1, 128.9, 126.6, 123.9, 123.2, 122.8, 122.2, 120.6, 120.2, 119.8, 119.3, 112.9, 60.4, 52.8, 41.4, 34.3, 31.4; MS (MALDI-TOF): *m/z*: 1615.5 [M^+]; Calcd for $C_{104}H_{98}N_{10}O_8$ (*m/z*): 1615.9; IR (KBr) [cm^{-1}] 3418 (N–H), 3056 (C–H), 2958 (C–H), 2866 (C–H), 1707 (C=O), 1671 (C=O), 1589 (C=C, perylene ring).

Acknowledgements

Financial support from the Natural Science Foundation of China (Grant No. 20640420476, 20771066), Ministry of Education of China, and Shandong University are gratefully acknowledged. We also thank the Deutsche Forschungsgemeinschaft and the Fond der Chemischen Industrie for funding.

References

1 (*a*) A. W. Czarnik, *Fluorescent Chemosensors for Ion and Molecule Recognition*, A.C.S., Washington DC, 1992; (*b*) C. D. Geddes, J. R. Lakowicz, *Advanced Concepts in Fluorescence Sensing Part A: Small Molecule Sensing*, Springer, New York, 2005; (*c*) A. P. de Silva, H. Q. N. Gunaratne, T. Gunnlaugsson, A. J. M. Huxley, C. P. McCoy, J. T. Rademacher and T. E. Rice, *Chem. Rev.*, 1997, **97**, 1515–1566; (*d*) A. P. de Silva, D. B. Fox, A. J. M. Huxley and T. S. Moody, *Coord. Chem. Rev.*, 2000, **205**, 41–57; (*e*) C. Bargossi, M. C. Fiorini, M. Montalti, Prodi L. Prodi and N. Zaccheroni, *Coord. Chem. Rev.*, 2000, **208**, 17–32; (*f*) L. F. Bolletta, M. Montalti and N. Zaccheroni, *Coord. Chem. Rev.*, 2000, **205**, 59–83; (*g*) D. T. McQuade, A. E. Pullen and T. M. Swager, *Chem. Rev.*, 2000, **100**, 2537–2574; (*h*) K. Rurack, *Spectrochim. Acta, Part A*, 2001, **57**, 2161–2195; (*i*) P. Jiang and Z. Guo, *Coord. Chem. Rev.*, 2004, **248**, 205–229; (*j*) J. F. Callan, A. P. de Silva and D. C. Magri, *Tetrahedron*, 2005, **61**, 8551–8588; (*k*) T. Gunnlaugsson, M. Glynn, G. M. Tocci (née Hussey), P. E. Kruger and F. M. Pfeffer, *Coord. Chem. Rev.*, 2006, **250**, 3094–3117; (*l*) J. S. Kim and D. T. Quang, *Chem. Rev.*, 2007, **107**, 3780–3799; (*m*) E. M. Nolan and S. J. Lippard, *Chem. Rev.*, 2008, **108**, 3443–3480.

2 (*a*) A. P. de Silva, T. Gunnlaugsson and T. E. Rice, *Analyst*, 1996, **121**, 1759–1762; (*b*) A. P. de Silva, H. Q. N. Gunaratne, T. Gunnlaugsson, C. P. McCoy, P. R. S. Maxwell, J. T. Rademacher and T. E. Rice, *Pure Appl. Chem.*, 1996, **68**, 1443–1448; (*c*) A. P. de Silva, H. Q. N. Gunaratne and C. P. McCoy, *Chem. Commun.*, 1996, 2399–2400; (*d*) R. Krämer, *Angew. Chem., Int. Ed.*, 1998, **37**, 772–773; (*e*) L. Fabbrizzi, M. Licchelli, L. Parodi, A. Poggi and A. Taglietti1, *J. Fluoresc.*, 1998, **8**, 263–271; (*f*) S. L. Wiskur, H. Ait-Haddou, J. J. Lavigne and E. V. Anslyn, *Acc. Chem. Res.*, 2001, **34**, 963–972.

3 (*a*) R. A. Bissell, A. P. de Silva, H. Q. N. Gunaratne, P. L. M. Lynch, E. G. E. M. Maguire, C. P. McCoy and K. R. A. S. Sandanayake, *Chem. Soc. Rev.*, 1992, **21**, 187–195; (*b*) R. A. Bissell, A. P. de Silva, H. Q. N. Gunaratne, P. L. M. Lynch, E. G. E. M. Maguire, C. P. McCoy and K. R. A. S. Sandanayake, *Top. Curr. Chem.*, 1993, **168**, 223–264; (*c*) A. P. de Silva, H. Q. N. Gunaratne and C. P. McCoy, *J. Am. Chem. Soc.*, 1997, **119**, 7891–7892; (*d*) A. J. Bryan, A. P. de Silva, S. A. De Silva, R. A. D. D. Rupasinghe and K. R. A. S. Sandanayake, *Biosensors*, 1989, **4**, 169–179; (*e*) A. P. de Silva, S. A. de Silva, A. S. Dissanayake and K. R. A. S. Sandanayake, *J. Chem. Soc., Chem. Commun.*, 1989, 1054–1056; (*f*) A. W. Czarnik, *Acc. Chem. Res.*, 1994, **27**, 302–308; (*g*) L. Prodi, F. Bolletta, N. Zaccheroni, C. I. F. Watt and N. J. Mooney, *Chem.–Eur. J.*, 1998, **4**, 1090–1094; (*h*) K. A. Mitchell, R. G. Brown, D. Yuan, S.-C. Chang, R. E. Utecht and D. E. Lewis, *J. Photochem. Photobiol., A*, 1998, **115**, 157–161; (*i*) C.-T. Chen and W.-P. Huang, *J. Am. Chem. Soc.*, 2002, **124**, 6246–6247; (*j*) H. He, M. A. Mortellaro, M. J. P. Leiner, S. T. Young, R. J. Fraatz and J. K. Tusa, *Anal. Chem.*, 2003, **75**, 549–555; (*k*) S. Aoki, S. Kaido, H. Fujioka and E. Kimura, *Inorg. Chem.*, 2003, **42**, 1023–1030; (*l*) X. Guo, X. Qian and L. Jia, *J. Am. Chem. Soc.*, 2004, **126**, 2272–2273; (*m*) T. Schwarze, H. Müller, C. Dosche, T. Klamroth, W. Mickler, A. Kelling, H.-G. Löhmannsröben, P. Saalfrank and H.-J. Holdt, *Angew. Chem., Int. Ed.*, 2007, **46**, 1671–1674; (*n*) J. S. Kim and D. T. Quang, *Chem. Rev.*, 2007, **107**, 3780–3799; (*o*) E. M. Nolan and S. J. Lippard, *Chem. Rev.*, 2008, **108**, 3443–3480; (*p*) J. Huang, Y. Xu and X. Qian, *J. Org. Chem.*, 2009, **74**, 2167–2170; (*q*) N. C. Lim, S. V. Pavlova and C. Bruckner, *Inorg. Chem.*, 2009, **48**, 1173–1182.

4 (*a*) M. R. Wasielewski, *J. Org. Chem.*, 2006, **71**, 5051–5066; (*b*) J. A. A. W. Elemans, R. van Hameren, R. J. M. Nolte and A. E. Rowan, *Adv. Mater.*, 2006, **18**, 1251–1266; (*c*) H. Langhals, *Helv. Chim. Acta*, 2005, **88**, 1309–1343; (*d*) F. Würthner, *Chem. Commun.*, 2004, 1564–1579.

5 (*a*) J. Feng, B. Liang, D. Wang, L. Xue and X. Li, *Org. Lett.*, 2008, **10**, 4437–4440; (*b*) C. Zhao, Y. Zhang, R. Li, X. Li and J. Jiang, *J. Org. Chem.*, 2007, **72**, 2402–2410; (*c*) W. Xu, H. Chen, Y. Wang, C. Zhao, X. Li, S. Wang and Y. Weng, *ChemPhysChem*, 2008, **9**, 1409–1415; (*d*) B. A. Jones, M. J. Ahrens, M.-H. Yoon, A. Facchetti, T. J. Marks and M. R. Wasielewski, *Angew. Chem., Int. Ed.*, 2004, **43**, 6363–6366; (*e*) K. Muthukumaran, R. S. Loewe, C. Kirmaier, E. Hindin, J. K. Schwartz, I. V. Sazanovich, J. R. Diers, D. F. Bocian, D. Holten and J. S. Lindsey, *J. Phys. Chem. B*, 2003, **107**, 3431–3442; (*f*) C. Kirmaier, E. Hindin, J. K. Schwartz, I. V. Sazanovich, J. R. Diers, K. Muthukumaran, M. Taniguchi, D. F. Bocian, J. S. Lindsey and D. Holten, *J. Phys. Chem. B*, 2003, **107**, 3443–3454.

6 (*a*) X. Guo, D. Zhang and D. Zhu, *Adv. Mater.*, 2004, **16**, 125–130; (*b*) Y. Li, N. Wang, H. Gan, H. Liu, H. Li, Y. Li, X. He, C. Huang, S. Cui, S. Wang and D. Zhu, *J. Org. Chem.*, 2005, **70**, 9686–9692; (*c*) Y. Li, H. Zheng, Y. Li, S. Wang, Z. Wu, P. Liu, Z. Gao, H. Liu and D. Zhu, *J. Org. Chem.*, 2007, **72**, 2878–2885; (*d*) X. He, H. Liu, Y. Li, S. Wang, Y. Li, N. Wang, J. Xiao, X. Xu and D. Zhu, *Adv. Mater.*, 2005, **17**, 2811–2815.

7 (*a*) H.-W. Rhee, C.-R. Lee, S.-H. Cho, M.-R. Song, M. Cashel, H. E. Choy, Y.-J. Seok and J.-I. Hong, *J. Am. Chem. Soc.*, 2008, **130**, 784–785; (*b*) H. M. Kim, M. S. Seo, M. J. An and B. R. Cho, *Angew. Chem.*, 2008, **120**, 5245–5248; (*c*) X. Peng, J. Du, J. Fan, J. Wang, Y. Wu and J. Zhao, *J. Am. Chem. Soc.*, 2007, **129**, 1500–1501; (*d*) J. Y. Kwon, Y. J. Jang, Y. J. Lee, K. M. Kim, M. S. Seo, W. Nam and J. Yoon, *J. Am. Chem. Soc.*, 2005, **127**, 10107–10111; (*e*) K. Komatsu, K. Kikuchi, H. Kojima, Y. Urano and T. Nagano, *J. Am. Chem. Soc.*, 2005, **127**, 10197–10204; (*f*) A. Ojida, Y. Mito-oka, K. Sada and I. Hamachi, *J. Am. Chem. Soc.*, 2004, **126**, 2454–2463; (*g*) T. Hirano, K. Kikuchi, Y. Urano and T. Nagano, *J. Am. Chem. Soc.*, 2002, **124**, 6555–6562; (*h*) S. C. Burdette, G. K. Walkup, B. Spingler, R. Y. Tsien and S. J. Lippard, *J. Am. Chem. Soc.*, 2001, **123**, 7831–7841; (*i*) T. Hirano, K. Kikuchi, Y. Urano, T. Higuchi and T. Nagano, *J. Am. Chem. Soc.*, 2000, **122**, 12399–12400; (*j*) Z. Liu, C. Zhang, Y. Li, Z. Wu, F. Qian, X. Yang, W. He, X. Gao and Z. Guo, *Org. Lett.*, 2009, **11**, 795–798; (*k*) E. Ballesteros, D. Moreno, T. Gómez, T. Rodríguez, J. Rojo, M. García-Valverde and T. Torroba, *Org. Lett.*, 2009, **11**, 1269–1272; (*l*) S. Atilgan, T. Ozdemir and E. U. Akkaya, *Org. Lett.*, 2008, **10**, 4065–4067; (*m*) J. D. Amilan, M. Sandhya and G. Amrita, *Org. Lett.*, 2007, **9**, 1979–1982; (*n*) X. Zhang, K. S. Lovejoy, A. Jasanoff and S. J. Lippard, *Proc. Natl. Acad. Sci. U. S. A.*, 2007, **104**, 10780–10785; (*o*) S. A. de Silva, A. Zavaleta, D. E. Baron, O. A. Edward, V. Isidor, N. Kashimura and J. M. Percarpio, *Tetrahedron Lett.*, 1997, **38**, 2237–2240; (*p*) P. Arslan, F. D. Virgilio, M. Beltrame, R. Y. Tsien and T. Pozzan, *J. Biol. Chem.*, 1985, **260**, 2719–2727; (*q*) G. Anderegg and F. Wenk, *Helv. Chim. Acta*, 1967, **50**, 2330–2332; (*r*) S. Banthia and A. Samanta, *New J. Chem.*, 2005, **29**, 1007–1010.

8 R. H. Goldsmith, L. E. Sinks, R. F. Kelley, L. J. Betzen, W. Liu, E. A. Weiss, M. A. Ratner and M. R. Wasielewski, *Proc. Natl. Acad. Sci. U. S. A.*, 2005, **102**, 3540–3545.

9 J. Feng, Y. Zhang, C. Zhao, R. Li, W. Xu, X. Li and J. Jiang, *Chem.–Eur. J.*, 2008, **14**, 7000–7010.

10 (*a*) J. Feng, B. Liang, D. Wang, H. Wu, L. Xue and X. Li, *Langmuir*, 2008, **24**, 11209–11215; (*b*) Z. Chen, U. Baumeister, C. Tschierske and F. Würthner, *Chem.–Eur. J.*, 2007, **13**, 450–465; (*c*) F. Würthner, C. Thalacker, S. Diele and C. Tschierske, *Chem.–Eur. J.*, 2001, **7**, 2245–2253; (*d*) F. Würthner, C. Thalacker, A. Sautter, W. Schärtl, W. Ibach and O. Hollricher, *Chem.–Eur. J.*, 2000, **6**, 3871–3886; (*e*) T. E. Kaiser, H. Wang, V. Stepanenko and F. Würthner, *Angew. Chem.*, 2007, **119**, 5637–5640; (*f*) Pascal. Jonkheijm, N. Stutzmann, Z. Chen, D. M. de Leeuw, E. W. Meijer, A. P. H. J. Schenning and F. Würthner, *J. Am. Chem. Soc.*, 2006, **128**, 9535–9540; (*g*) F. Würthner, Z. Chen, F. J. M. Hoeben, P. Osswald, C.-C. You, P. Jonkheijm, J. V. Herrikhuyzen, A. P. H. J. Schenning, P. P. A. M. van der Schoot, E. W. Meijer, E. H. A. Beckers, S. C. J. Meskers and R. A. J. Janssen, *J. Am. Chem. Soc.*, 2004, **126**, 10611–10618; (*h*) F. Würthner, *Chem. Commun.*, 2004, 1564–1579.

11 R. Gvishi, R. Reisfeld and Z. Burshtein, *Chem. Phys. Lett.*, 1993, **213**, 338–344.

12 (*a*) T. L. Banfield and D. Husain, *Trans. Faraday Soc.*, 1969, **65**, 1985–1991; (*b*) A. W. Varnes, R. B. Dodson and E. L. Wehry, *J. Am. Chem. Soc.*, 1972, **94**, 946–950.
13 J. K. Romary, J. D. Barger and J. E. Bunds, *Inorg. Chem.*, 1968, **7**, 1142–1145.
14 (*a*) S. Foxon, J. Xu, S. Turba, M. Leibold, F. Hempel, F. W. Heinemann, O. Walter, C. Würtele, M. Holthausen and S. Schindler, *Eur. J. Inorg. Chem.*, 2007, 429–443; (*b*) A. Hazell, C. J. McKenzie and L. P. Nielsen, *J. Chem. Soc., Dalton Trans.*, 1998, 1751–1756.
15 A. Hazell, C. J. McKenzie and L. P. Nielsen, *Polyhedron*, 2000, **19**, 1333–1338.
16 (*a*) H. A. Benesi and J. H. Hildebrand, *J. Am. Chem. Soc.*, 1949, **71**, 2703–2707; (*b*) W. Qin, M. Baruah, M. Sliwa, M. V. der Auweraer, W. M. De Borggraeve, D. Beljonne, B. V. Averbeke and N. Boens, *J. Phys. Chem. A*, 2008, **112**, 6104–6114; (*c*) Y. Shiraishi, S. Sumiya, Y. Kohno and T. Hirai, *J. Org. Chem.*, 2008, **73**, 8571–8574.
17 (*a*) B. Ramachandram and A. Samanta, *Chem. Commun.*, 1997, 1037–1038; (*b*) S. Banthia and A. Samanta, *J. Phys. Chem. B*, 2002, **106**, 5572–5577.
18 K. Rurack and U. Resch-Genger, *Chem. Soc. Rev.*, 2002, **31**, 116–127.
19 P. Ghosh, P. K. Bharadwaj, S. Mandal and S. Ghosh, *J. Am. Chem. Soc.*, 1996, **118**, 1553–1554.
20 X. Zhang, Y. Shiraishi and T. Hirai, *Org. Lett.*, 2007, **9**, 5039–5042.
21 (*a*) J. L. Bricks, A. Kovalchuk, C. Trieflinger, M. Nofz, M. Büschel, A. I. Tolmachev, J. Daub and K. Rurack, *J. Am. Chem. Soc.*, 2005, **127**, 13522–13529; (*b*) Y. Xiang and A. Tong, *Org. Lett.*, 2006, **8**, 1549–1552; (*c*) J. Mao, L. Wang, W. Dou, X. Tang, Y. Yan and W. Liu, *Org. Lett.*, 2007, **9**, 4567–4570; (*d*) X. Zhang, Y. Shiraishi and T. Hirai, *Tetrahedron Lett.*, 2008, **49**, 4178–4181; (*e*) N. C. Lim, S. V. Pavlova and C. Brückner, *Inorg. Chem.*, 2009, **48**, 1173–1182; (*f*) W. Lin, L. Long, L. Yuan, Z. Cao and J. Feng, *Anal. Chim. Acta*, 2009, **634**, 262–266.
22 F. Würthner, A. Sautter and J. Schilling, *J. Org. Chem.*, 2002, **67**, 3037–3044.
23 J. Wang, Y. Xiao, Z. Zhang, X. Qian, Y. Yang and Q. Xu, *J. Mater. Chem.*, 2005, **15**, 2836–2839.
24 M. G. Ferlin, L. Dalla Via and O. M. Gia, *Bioorg. Med. Chem.*, 2004, **12**, 771–777.
25 V. Percec, C.-H. Ahn, T. K. Bera, G. Ungar and D. J. P. Yeardley, *Chem.–Eur. J.*, 1999, **5**, 1070–1083.

